Multifunctional Acrylic-Based Nanocomposites for Protecting Heritage Textiles

Nabil Mabrouk
Faculty of Archaeology, Damietta University
nsh00@du.edu.eg

ARTICLE INFO
Article history
Received 10 December 2024
Received in revised form 7 February 2025
Accepted 28 February 2025
Available Online 18 June 2025

KEYWORDS
Ag-SiO2; S-SiO2; Multifunctional; Nanocomposite; Heritage Textile

ABSTRACT
The present study aims to assess two nanocomposites (S-SiO_2 and Ag-SiO_2) suspended in two copolymers (Beva 371 and Paraloid B72) for their efficiency in consolidation, UV-blocking, and antimicrobial activities against six fungi and six bacteria, applied to dyed silk fabric samples. TEM, SEM-EDX, XRD, UTM, colorimeter, stiffness tester, air permeability, and inhibition zone techniques were used. The obtained results demonstrated the successful preparation of both nanocomposites. All treatments had varying positive and negative effects on the properties of silk fabrics. The more nanomaterials, the greater the effects on the samples' properties. Paraloid-based treatments exhibited more improvement in all fabrics' properties but increased the stiffness differently. On the contrary, Beva-based treatments showed better results in terms of elongation percentage and flexibility of the samples. The Ag-based treatments exhibited better results than the S-based treatments in anti-UV and antimicrobial activities against the tested fungi and bacteria. The concentration of 600 µg/mL of Ag-SiO_2 nanocomposite in 2% Paraloid B72 in toluene is recommended as a multifunctional formula for consolidating, UV-blocking, and antimicrobial activity of stiff and/or thick heritage textiles and carpets, whilst the 600 µg/mL of Ag-SiO_2 nanocomposite in 2% Beva 371 in toluene is recommended as a multifunctional formula for the fine and delicate heritage textiles.

INTRODUCTION

Cultural heritage is a non-renewable resource of human history. It is a complex set of materials that belongs to all humanity, not just individual cultures. It has survived thousands of years due to its materials' durability and the fewer deterioration factors in its environment (Elkadi et al., 2021; Samadelli et al., 2019). Natural deterioration is the main cause of damage to heritage objects (Samadelli et al., 2019), which is an unavoidable result of the life-cycle of heritage objects, despite working to interrupt this process, or at least to slow it down (Kavkler et al., 2014). These heritage objects were used by ancient people and weren't fabricated to last a long time. Therefore, preservation can be achieved by using many preventive procedures to create a suitable and safe environment for the heritage objects (Kavkler et al., 2014; Lucchi, 2018).

Chemical deterioration can occur due to photochemical reactions, resulting in damage, such as fading and yellowing, when exposed to light (Michalski, 2018). High temperatures cause textiles to become dry and brittle due to dehydration (Brimblecombe & Lankester, 2013; Tétreault, 2003). The rise of relative humidity results in the expansion of the heritage textiles, after which the textiles start to shrink due to a decrease in humidity (Bratasz et al., 2015). Because high relative humidity induces physical, chemical, and biological deterioration, its damage is more destructive to heritage objects than high temperatures. The higher the relative humidity, the higher the potential for microbial growth (Guo et al., 2023; Maekawa et al., 2015).

Heritage objects of organic materials are more susceptible to microorganisms. In the bio-deterioration process of heritage textiles, microorganisms can excrete destructive enzymes (e.g., extracellular cellulolytic and proteolytic enzymes), pigments, and acids (Gutarowska et al., 2017; Johansson et al., 2010). Fungi found on textiles include many species, e.g., *Acremonium, Alternaria, Aspergillus, Aureobasidium, Cephalothecium, Chaetomium, Chrysosporium, Cladosporium, Dematium, Fusarium, Memnoniella, Microsporum, Mucor, Myrothecium, Oospora, Paecilomyces, Penicillium, Rhizopus, Scopulariopsis, Stachybotrys, Trichoderma, Trichophyton, Trichothecium, Ulocladium,* and *Verticillium*. Bacteria found on textiles include *Aeromonas, Alcaligenes, Arthrobacter, Bacillus, Cellulomonas, Cellvibrio, Chryseomonas, Clostridium, Cytophaga, Microbispora, Nocardia, Proteus, Pseudomonas, Serratia, Sporocytophaga, Streptomyces,* and *Variovorax* (Omar Abdel-Kareem, 2010; O. Abdel-Kareem, 2010; Błyskal, 2015; Forlani et al., 2000; Montegut et al., 1991; Ramasamy, 2019; Szostak-Kotowa, 2004; Sülar & Devrim, 2019).

Early practices in heritage science involved strengthening degraded textiles with natural resins, followed by synthetic and semi-synthetic ones. These resins had initially stabilized the objects, but almost induced degradation (De Witte, 1982). Acrylic resins proved good adhesive properties and moderate water repellence (Princi et al., 2005). For example, Beva 371, Paraloid B72, and Plexisol P550 were used in heritage textiles and canvas consolidation (Ezz Eldeen et al., 2020; Oriola-Folch et al., 2020). Studies have addressed the microbial infections of heritage textiles, and different physical, mechanical, and biochemical methods of disinfection, such as scalpels, spatulas, and vacuum cleaners (Munichia et al., 2018), low frequency systems, heat, and UV radiation (Scheerer et al., 2009), gamma irradiation (del Carmen Calvo et al., 2017), as well as chemicals, such as phenol, aldehydes, acids, amides, and alcohol (Singer et al., 2010), fumigation with ethylene oxide (Nugari & Salvadori, 2017), and vaporized hydrogen peroxide (Anna et al., 2020).

Some nanoparticles (NPs), as a novel branch of heritage science, can change the characteristics of the cell membrane in microorganisms, cause damage to DNA, and release toxic ions; thus, they have been widely used in the conservation of historical and cultural heritage. Other NPs can block UV radiation. To enhance antimicrobial efficiency and UV-blocking properties, different NPs, such as silver (Ag), titanium oxide (TiO_2), copper (Cu), and zinc oxide (ZnO), are commonly used (Jia et al., 2019; Morones et al., 2005; Ruparelia et al., 2008). Polymer nanocomposites (PNCs) are a novel method used to describe polymers or copolymers reinforced with nanomaterials dispersed in their matrix. PNCs play a multifunctional role in textiles conservation as consolidants and protect materials against harmful environmental and microbial factors (Abdel-Kareem et al., 2015). Recent studies have focused on using polyvinyl acetate (PVA)/nanocellulose reinforced with silicon dioxide (SiO_2) NPs to increase the paper's tensile strength (Ching et al., 2015).

SiO_2-NPs are readily available, non-toxic, and inexpensive material. It has been used in paper, painting, and pigment consolidation due to the addition of polymers, such as PVA and nanocellulose (Ching et al., 2015; Palladino et al., 2020). Sulfur nanoparticles (S-NPs) are commonly used in various applications, particularly in antibacterial and antifungal applications

 DOI: 10.21608/shedet.2025.386138.1302

(Rai et al., 2016; Sadek et al., 2022). S-NPs (concentration range: 10 to 500 mM) exhibit more potent activity against Gram-negative, Gram-positive, yeast, and fungal pathogens (Kim et al., 2020). Ag-NPs are also common nanomaterials that have been widely used against the biodeterioration affecting textile objects, especially *E. coli, B. subtilis, P. aeruginosa,* and *K. pneumoniae* (Perkas et al., 2007; Ruparelia et al., 2008).

This study introduces a novel approach to the application of multifunctional acrylic-based nanocomposites in the preventive conservation of heritage textiles. For the first time, S-NPs and Ag-NPs are separately loaded onto SiO_2-NPs and then mixed in acrylic copolymer (Beva 371 or Paraloid B72). These formulas are designed to achieve three objectives: strengthening, antimicrobial, and anti-UV activities, due to their unique properties, including radical and heavy metal scavenging, antimicrobial, and antioxidant activities.

1. MATERIALS AND METHODS

1.1. Materials

Scoured and unbleached creamy silk fabric from the local market was used in the preparation of fabric mock-ups. The number of threads was 46 warp and 50 wefts in cm. Weight was 75 g/m^2. The weave structure was plain 1/1. Madder roots and alum, purchased from Harraz (Agricultural, Seeds Medicinal plant Company), were used to mordant the fabric with a red dye. Additionally, Beva 371 and Paraloid B72 (CTS, Italy) were used as consolidating copolymers, dissolved in pure toluene (Sigma-Aldrich, USA), reinforced with the prepared nanomaterials as explained below. Sodium metasilicate (SMS), cetyltrimethylammonium bromide (CTAB), tetraethyl orthosilicate TEOS, sodium hydroxide NaOH, sodium chloride, silver nitrate $AgNO_3$, oxalic acid, HCl (37%), and analytical-grade ethyl alcohol EtOH (Sigma-Aldrich) were used to prepare nanocomposite materials**.** Nutrient agar (NA) and potato dextrose agar (PDA) (Sigma-Aldrich, USA) were used as media for bacterial growth and fungal growth, respectively, to identify the antifungal and antibacterial activities of each treatment in different concentrations.

1.2. Preparation of silk fabric mock-ups (SFMs)

The silk fabric was immersed and stirred in hot water mixed with soap for 30 min. at 60°C. It was then repeatedly rinsed in distilled water and dried in an oven at 50°C (ASTM-D629, 1999). The madder roots were soaked in water (ratio of 1:10) at room temperature for 12 hrs., then heated at 90ºC for 60 min. After that, they were filtered and cooled (Goodarzian & Ekrami, 2010). A mordant bath (2.5 g of alum in 1,000 mL of water) was prepared at 80ºC for 30 min. The fabric was immersed and stirred for 30 min. Next, the mordanted fabric was rinsed and dried, then immersed and stirred in the dye bath at 80ºC for 30 min., and after that rinsed in water and dried (Bechtold et al., 2003; Grifoni et al., 2011; Schweppe, 1988). The silk fabric was cut into mock-ups (SFMs) according to the required size in each test, then thermally aged (Binder ED115, Germany) at 125 °C for 21 days, to create fiber properties similar to the naturally aged silk heritage textiles (Vilaplana et al., 2015).

1.3. Preparation of nanocomposites

1.3.1. Synthesis of S-SiO_2 nanocomposite

Microporous SiO_2-NPs were fabricated following the wet-gel method (Abou Abou Rida & Harb, 2014) by stirring 8 g CTAB in 400 mL SMS at a concentration of 1.5% at 55°C. After that, the mixture was mixed with HCl (2.5%) by adding HCl dropwise until semigelation at pH 9-9.5, and then stirred for 10 min. Next, HCl was readded until the pH reached 3 to 3.5. Next, 10 mL sodium chloride (10%) was added with stirring for 20 min. The wet gel was incubated at 50°C for 24 hrs., then washed using distilled water and centrifuged at 4000 rpm. The wet gel was then dried in a microwave oven, followed by calcination for 3 hrs. at 650°C in a muffle, and then milled into a fine powder. After that, 0.5 g of SiO_2-NPs and 1 g of $Na_2S_2O_3.5H_2O$ were milled in an agate mortar. The mixture was then kept for 24 hrs. for the adsorption of the

S precursor on the surface of SiO_2. Finally, 0.508 g of oxalic acid was added and ground for 30 min. The obtained S-SiO_2 powder was stored at 4°C until use.

1.3.2. Synthesis of Ag-SiO_2 nanocomposite

Solution (1): 0.25 g $AgNO_3$ was dissolved in 50 mL deionized water under stirring. Solution (2): 0.35 g $NaBH_4$, 0.14 g PVP, 10 mL 0.4% NaOH, and 120 mL ethanol. Solution (2) was slowly added dropwise via a micropipette into solution (1) within 10 min. to form an Ag-NPs colloid. After that, 0.25 g APTES, 1.15 g CTAB, 50 mL ethanol, 2.5 mL TEOS, and 5 mL ammonia were slowly added dropwise via a micropipette to the colloid of Ag-NPs. The mixture was then stirred at 25°C for 2 hrs. Centrifugation for 10 min. at 8000 rpm was conducted to collect the Ag-SiO_2 nanocomposite after washing with ethanol and deionized water, and then dried in a freeze dryer under vacuum, resulting in a yellowish Ag-SiO_2 core-shell powder (Ye et al., 2024).

1.4. Preparation of acrylic-based nanocomposites (ABNCs):

1.4.1. Beva 371-based nanocomposites

The first ABNC was based on using the S-SiO_2-NPs in 2% Beva 371 (B-S-SiO_2). The S-SiO_2-NPs were suspended in Beva 371 solutions in different concentrations (200, 400, 600, and 800 µg/mL). The second ABNC was based on using the Ag-SiO_2 core-shell nanocomposite in 2% Beva 371 (B-Ag-SiO_2). The Ag-SiO_2 core-shell nanocomposite was suspended in Beva 371 solutions in different concentrations (200, 400, 600, and 800 µg/mL). After the suspension of each nanocomposite (S-SiO_2 and Ag-SiO_2) in each 1mL of 2% Beva 371 solution to form each required ABNC (B-S-SiO_2, B-Ag-SiO_2), each mixture was sonicated using ultrasonic magnetic stirring (Elmasonic S S30H, Germany) at 22ºC for 30 min. to ensure the complete uniform distribution of the nanoparticles in the copolymer (Elsayed, 2025; Ye et al., 2024). The SFMs were then immersed in the ABNCs at 22ºC for 1 min. under sonication, then dried and kept for 72 hrs. (Yong-hua et al., 2012).

1.4.2. Paraloid B72-based nanocomposites

The third ABNC was based on using the S-SiO_2 nanocomposite in 2% Paraloid B72 (P-S-SiO_2). The S-SiO_2 nanocomposite was suspended in Paraloid B72 solutions in different concentrations (200, 400, 600, and 800 µg/mL). The fourth ABNC was based on an Ag-SiO_2 core-shell nanocomposite in Paraloid B72 (P-Ag-SiO_2). The Ag-SiO_2 core-shell nanocomposite was suspended in Paraloid B72 solutions in different concentrations (200, 400, 600, and 800 µg/mL). After the suspension of each nanocomposite (S-SiO_2 and Ag-SiO_2) in each 1mL of 2% Paraloid solution to form each required ABNC (P-S-SiO_2, P-Ag-SiO_2), each mixture was sonicated using ultrasonic magnetic stirring (Elmasonic S S30H, Germany) at 22ºC for 30 min. to ensure the complete uniform distribution of the nanocomposite in the copolymer (Elsayed, 2025; Ye et al., 2024). The SFMs were then immersed in the ABNCs at 22ºC for 1 min. under sonication, then dried at room temperature (22ºC) for 24 hrs., and then kept for 72 hrs. (Yong-hua et al., 2012).

1.5. Accelerated aging of the SFMs-ABNCs

SFMs-ABNCs were exposed to accelerated aging to assess the sustainability and efficiency of the four treatments in terms of fiber consolidation, antimicrobial, and anti-UV activities for the long term. The SFMs-ABNCs were kept in the UV-weathering chamber (QUV-se, USA) for one month. The 24-hour weathering cycle consists of two steps: Step 1: UV radiation at 60 °C using eight UVA 340 nm lamps with an intensity of 1.5 W/m^2/nm, Step 2: the moisture condensation at 60°C. The SFMs-ABNCs were kept at 22ºC for 72 hrs. before measurements (Vilaplana et al., 2015; Yasuda et al., 2017). All details of the samples, before and after treatment and after UV-aging, are shown in Table 1 and Fig. 1.

 DOI: 10.21608/shedet.2025.386138.1302

Table.1 Silk samples before and after treatment and after UV-aging.

Untreated samples		Treated samples							
		Beva-S-SiO_2		Beva-Ag-SiO_2		Paraloid-S-SiO_2		Paraloid-Ag-SiO_2	
No.	ID	No.	Conc.	No.	Conc.	No.	Conc.	No.	Conc.
1	Blank (pre-dying)	Dyed, thermal-aged and treated samples							
2	Dyed	5	200 µg/mL	9	200 µg/mL	13	200 µg/mL	17	200 µg/mL
3	Thermal aged (pre-treat)	6	400 µg/mL	10	400 µg/mL	14	400 µg/mL	18	400 µg/mL
4	UV aged (post-treat)	7	600 µg/mL	11	600 µg/mL	15	600 µg/mL	19	600 µg/mL
		8	800 µg/mL	12	800 µg/mL	16	800 µg/mL	20	800 µg/mL
		Dyed, thermal-aged, treated, and UV-aged samples							
		21	200 µg/mL	25	200 µg/mL	29	200 µg/mL	33	200 µg/mL
		22	400 µg/mL	26	400 µg/mL	30	400 µg/mL	34	400 µg/mL
		23	600 µg/mL	27	600 µg/mL	31	600 µg/mL	35	600 µg/mL
		24	800 µg/mL	28	800 µg/mL	32	800 µg/mL	36	800 µg/mL

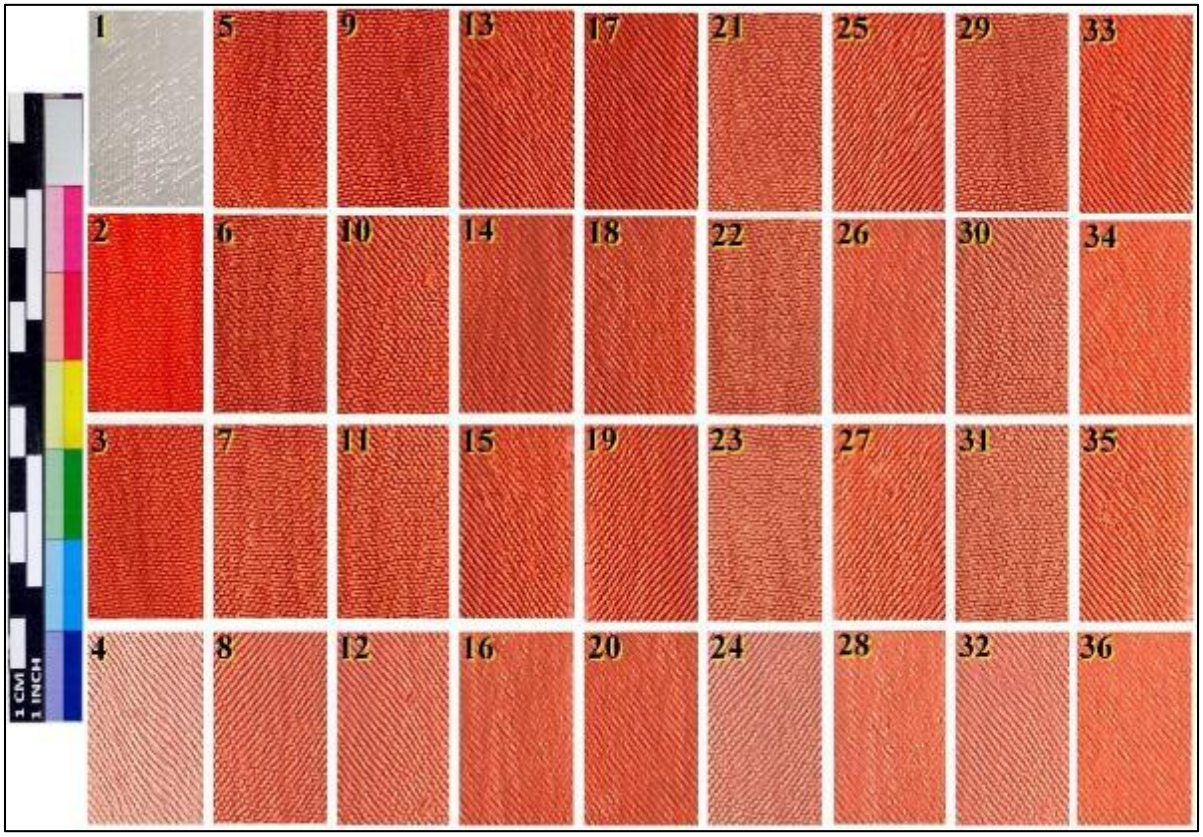

Fig. 1 Silk samples before and after treatment and after UV-aging.

1.6. Microbial strains and cultivation:

According to the literature (O. Abdel-Kareem, 2010; Brzozowska et al., 2018; De Leo & Isola, 2023; Forlani et al., 2000; Gutarowska et al., 2017; Kakakhel et al., 2019; Kavkler et al., 2015; Seves et al., 1998), *Aspergillus* spp., *Chaetomium* spp., *Penicillium* spp., *Alternaria* spp., *Cladosporium* spp., *Rhizopus* spp., *Trichoderma* spp., *Paecilomyces* spp., *Escherichia* spp., *Bacillus* spp., *Staphylococcus* spp., *Pseudomonas* spp., *Streptomyces* spp., *Salmonella* spp., *Enterococcus* spp., *Ornthinibacillus* spp., *zotobacter* spp., *Serratia* spp., *Aeromonas* spp., *Arthrobacter* spp., *Chryseomonas* spp., *Serratia* spp., and *Variovorax* spp. were the most common fungi and bacteria isolated from heritage textiles in different museums. Thus, the present study focused on six types of fungi (*Aspergillus niger*, *Aspergillus fumigatus*, *Cladosprium halotolerans*, *Penicillium frequentans*, *Alternaria alternata*, and *Rhizopus oryzae*), three gram-positive bacteria (*Bacillus cereus*, *Staphylococcus aureus*, *Streptomyces*

albus), and three gram-negative bacteria (*Escherichia coli*, *Pseudomonas aeruginosa*, and *Pseudomonas fluorescens*).

All types of microorganisms were supplied by the Department of Agricultural Biotechnology at Damietta University. (PDA) and (NA) were used as media for fungal growth and bacterial growth, respectively. Moreover, 5 mL of 0.09% NaCl sterilized saline solution was added to each slant. The cells were gently loosened by brushing with a sterile inoculating loop. To remove all microbial cells from the slants, a vortex mixer was used for 1 min. To determine the antimicrobial activity, Petri dishes containing 20 ml of NA medium each (El-Kadi et al., 2018a, pp. 5-11). Each SFMs-ABNCs (1cm×1cm) was placed above the microbial media. All fungal and bacterial strains were grown on PDA and NA slants and incubated at 30 °C and 37 °C, respectively. The inhibition zones were checked after 4 days and 1 day of fungal and bacterial incubation, respectively (Elsayed et al., 2023, pp. 127-143).

1.7. Characterization techniques:

1.7.1. X-ray diffraction (XRD)

To identify the crystalline nature and the chemical structure of the synthesized nanomaterials, an X-ray diffractometer (PANalytical Empyrean, Series 3, Netherlands) operating at Cu_Kα radiation 40 kV, 100 mA was used (Ye et al., 2024).

1.7.2. Scanning electron microscopy with energy dispersive X-ray spectroscopy (SEM-EDX)

The EDX attached to the scanning electron microscopy (JEOL JSM-6510LB, Tokyo, Japan) was used to characterize and confirm the chemical structure of the synthesized nanocomposites (Ye et al., 2024).

1.7.3. Transmission electron microscopy (TEM)

To characterize the morphology and size of the synthesized nanomaterials, a transmission electron microscope (JEOL, JEM 2100F, Tokyo, Japan) operating at 200 kV was used. A small sample of each nanomaterial was mixed in ethyl alcohol, put on a 400-mesh copper grid coated with a carbon film, and dried at 25 °C under vacuum (Elsayed & Sayed-Ahmed, 2024).

1.7.4. Color measurements

Color measurements of the SFMs-ABNCs were conducted to determine whether the studied treatments negatively affected the color properties of the silk fabric. The surface colors were measured using a colorimeter (PCE-CSM 2, PCE, Germany). Illuminant D65, SCI mode, 10° supplementary standard observer. L*, a*, b* were determined as a function of the CIEL*a*b 1976 color space. (ΔE∗) were calculated according to the equation: $\Delta E* = [(\Delta L*)^2 + (\Delta a*)^2 + (\Delta b*)^2]^{1/2}$ (Marchiafava et al., 2014, pp. 36-42).

1.7.5. Tensile strength and elongation%

The tensile strength and elongation% of the SFMs-ABNCs were conducted to clarify the improvement in the mechanical properties of the silk fabric samples after treatment with both Beva 371 and Paraloid B72, reinforced with the studied nanomaterials. A Universal testing machine (UTM) (Testometric XFS 150 KN, UK) was used according to ASTM (2000), D 5035-95. The test speed was 25 mm/min., the spacing of the initial jaw was 50 mm, at 22° C, and 65% relative humidity (ASTM International, 2004).

1.7.6. Stiffness test

A stiffness tester (Full-Automatic stiffness tester GT-C70A) was used to determine whether the ABNCs imparted any rigidity or stiffness to the SFMs due to using both copolymers (Sengupta et al., 2016). It is one of the most important criteria. The test was conducted according to ASTM D 1388. The sample size was 25×250 mm, the angle of the bevel was 45°, and the press plate speed was 0.4 cm/s.

 DOI: 10.21608/shedet.2025.386138.1302

1.7.7. Air permeability test

The automatic air permeability tester (GT-C27) was used to assess whether the ABNCs have any effect on the SFMs with respect to air permeability. The test was conducted at a pressure of 100 Pa, $cm^3/cm^2.s$ in accordance with ISO 9237 (Ogulata, 2006).

1.7.8. Weight test

A 4-decimal lab balance (OHAUS PR224, USA) was used to assess the weight of SFMs vs SFMs-ABNCs to clarify the weight increase limit after treatment.

2. RESULTS AND DISCUSSION

2.1. Results of nanomaterial characterization

The XRD and EDX spectra of the prepared nanocomposites (Fig. 2) confirmed the successful synthesis of both S-SiO_2 and Ag-SiO_2 nanocomposites, revealing the presence of the expected elements in the analyzed nanomaterials, namely oxygen (O), sulfur (S), silver (Ag), and silica (Si). The S-SiO_2 XRD spectrum (Fig. 2a) showed the presence of an amorphous silica peak at 20-26°, where sulfur appeared in the same region. It exhibited peaks well matched with the standard values of the orthorhombic phase of sulfur (JCPDS no. 08-0247) and matched with the literature (Alrefaee et al., 2024; Liu et al., 2020), as confirmed by the EDX results (Fig. 2c). Furthermore, the Ag-SiO_2 XRD spectrum (Fig. 2b) showed that Ag-NPs were successfully coated by SiO_2. The broad peak around 20–27° was assigned to the amorphous silica. Many distinct peaks appeared at 37.5°, 43.8°, 63.1°, and 76.3°, which were attributed to the Ag indices crystals (111), (200), (220), and (311) (Cai et al., 2024). The spectral results obtained by XRD and EDX were confirmed by TEM micrographs (Fig. 2e, f), which confirmed the successful preparation of both nanocomposites. S-SiO_2 nanocomposite exhibited a diameter average of ~50nm, whereas Ag-SiO_2 core-shell nanocomposite exhibited a diameter average of ~80nm, which confirmed the uniformity and the successful coating of Ag-NPs by SiO_2-NPs in accordance with the literature (Dhanalekshmi et al., 2019; Ye et al., 2024).

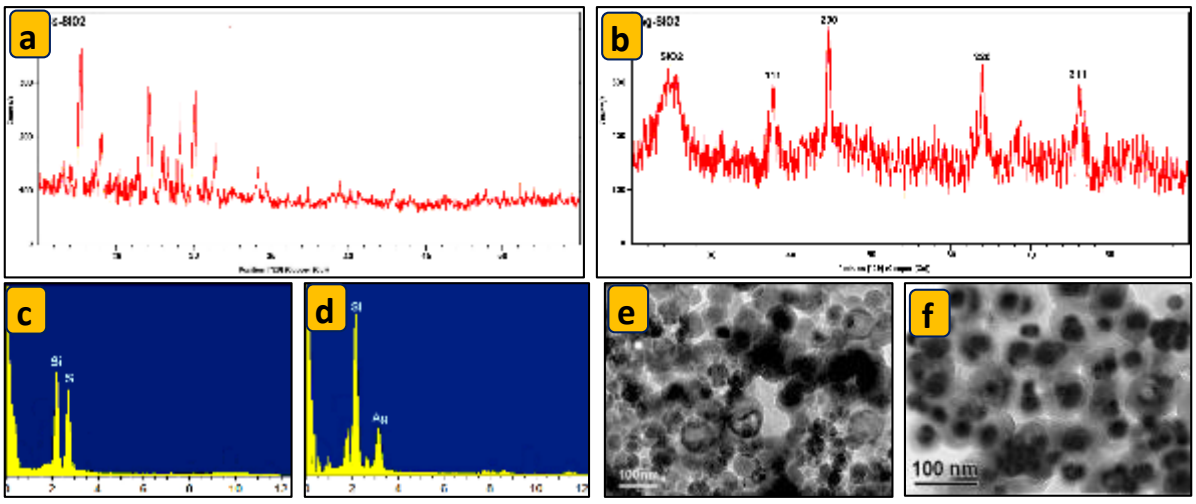

Fig. 2 characterization results of the studied nano composites, XRD spectra of; (a) S-SiO_2, (b) Ag-SiO_2, EDX spectra of; (c) S-SiO_2, (d) Ag-SiO_2, TEM micrographs of; (e) S-SiO_2, (f) Ag-SiO_2.

2.2. Results of silk-fabric characterization

One of the main terms and conditions in remedial conservation is to ensure that the anticipated treatment has no harmful effects on the properties of the treated object, in addition to its efficiency in achieving its main target, whether cleaning, consolidation, antimicrobial, anti-UV, etc. In this respect, many characterization techniques were applied to the silk-fabric samples before and after treatment steps as follows:

2.2.1. Mechanical properties

The obtained results of tensile strength (Fig. 3a), elongation% (Fig. 3b), and stiffness (Fig. 3c) of all treated samples revealed that all treatments increased all values of the tensile strength, elongation%, and stiffness of all samples in a variable ratio. The addition of nanomaterials improved the properties of the polymers (Emamhadi et al., 2020). Paraloid-based nanocomposites exhibited more tensile strength and stiffness, whilst Beva-based nanocomposites exhibited more elongation%, especially at the 800 µg/mL concentration. These results indicate that Paraloid B72 has a significant advantage, as it is a stronger and harder polymer compared to other polymers (Mandal et al., 2024). Moreover, the literature confirms that the addition of the nanoparticles, especially SiO_2, to the coating significantly increased the stiffness of the treated samples (Mahović Poljaček et al., 2021).

The increase of both tensile strength and elongation% values is attributed to the capability of polymers to improve the fibers' cohesion, whilst the decrease in these values after aging is normally attributed to the varying degradative effect of aging factors on both polymer and fabric, as commonly confirmed in literature (Abdel-Kareem & Nasr, 2010; Al-Gaoudi et al., 2024; Ezz Eldeen et al., 2020; Ranakoti et al., 2022). In conclusion, a concentration of 800 µg/mL should be avoided due to its potential negative effects on the stiffness of all samples; therefore, it should be excluded from the antimicrobial assessments, and only concentrations of 200 µg/mL, 400 µg/mL, and 600 µg/mL will be assessed.

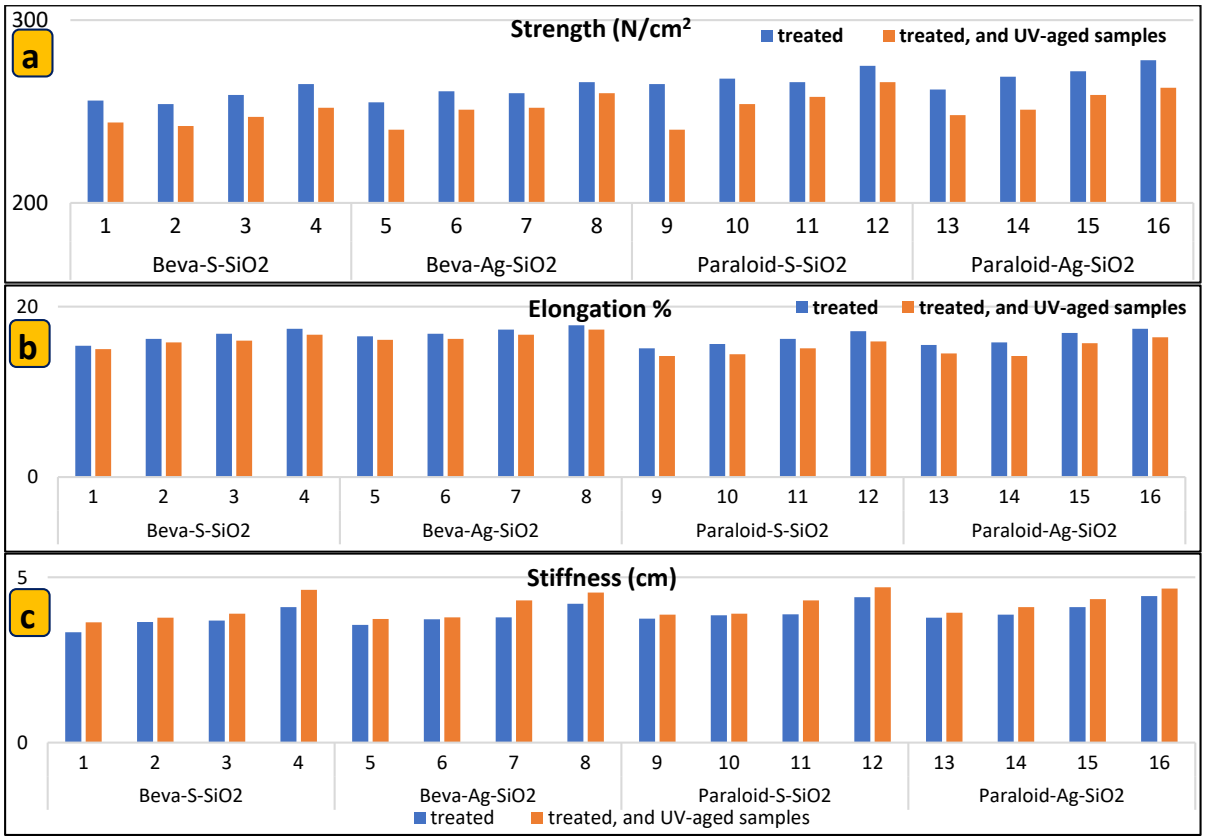

Fig. 3 Results of tensile strength N/cm² (a), elongation % (b), and stiffness cm (c) of treated samples and treated and UV-aged samples.

2.2.2. Physical properties

2.2.2.1. Color differences

The obtained pre- and post-treatment results of the silk-fabric samples (Fig. 4) revealed that both co-polymers (Beava 371 and Paraliod B72), reinforced with both nanocomposites (S-SiO_2 and Ag-SiO_2) at different concentrations (200, 400, 600, and 800 µg/mL), had variant effects

 DOI: 10.21608/shedet.2025.386138.1302

on the samples' colors. The color difference (ΔE) varied from 0 to 1 (not detectable by the human eye), and 1 to 3 (slight difference), no remarkable or large-variation differences (ΔE>3) were detected (Marchiafava et al., 2014; Schanda, 2007, pp. 79-91).

The results of the dyed, thermal-aged, and treated samples revealed that all samples were differently affected by the various treatments, especially the 800 µg/mL concentration. Despite the range of affection being generally low and somewhat accepted, the most affected group was the one treated with Beva-S-SiO_2, where ΔE reached 3.36 at 800 µg/mL concentration. In contrast, the less-affected group was that of Paraloid-Ag-SiO_2, where ΔE reached 0.47 at 200 µg/mL concentration. These results showed the somewhat heterogeneity in Beva-S-SiO_2 nanocomposite, if compared to Paraloid-Ag-SiO_2 nanocomposite, which commonly demonstrated suitability and efficiency in multi-applications of organic and inorganic heritage materials, especially if reinforced with nanomaterials (Aldoasri et al., 2018; Ion & Grigorescu, 2018; Mitani et al., 2024)

The results of the dyed, thermal-aged, and UV-aged samples revealed that all treatments protected the samples from harmful UV radiation compared to the untreated control sample (Degani et al., 2017; Vasileiadou et al., 2022). Despite the range of protection being generally high and promising, the most affected group was the one treated with Beva-S-SiO_2, as ΔE reached 4.11 in the case of the lowest concentration (200 µg/mL). In contrast, the most protected group was that of Paraloid-Ag-SiO_2, where ΔE reached 0.37 at the highest concentration (800 µg/mL).

These results proved that the samples' protection against UV could be attributed to the role of SiO_2, which proved high efficiency against UV radiation (Al-Gaoudi et al., 2024; Mahović Poljaček et al., 2021), in addition to the greater suitability of Paraloid B72-based nanocomposite in these treatments, due to the high stability of Paraloid B72 regardless of aging type (Krejčí et al., 2021). The effect of UV radiation on the silk fabric dyed with madder is affected by many parameters, such as mordants and their technique, the type of fiber, the amount of dye, the source dyestuff, and the conditions of ageing procedures (Vasileiadou et al., 2022). In sum, the concentration of 800 µg/mL is not suitable due to its high negative effects on color, particularly those based on Beva. It proved to be displaceable, despite having high antimicrobial activity.

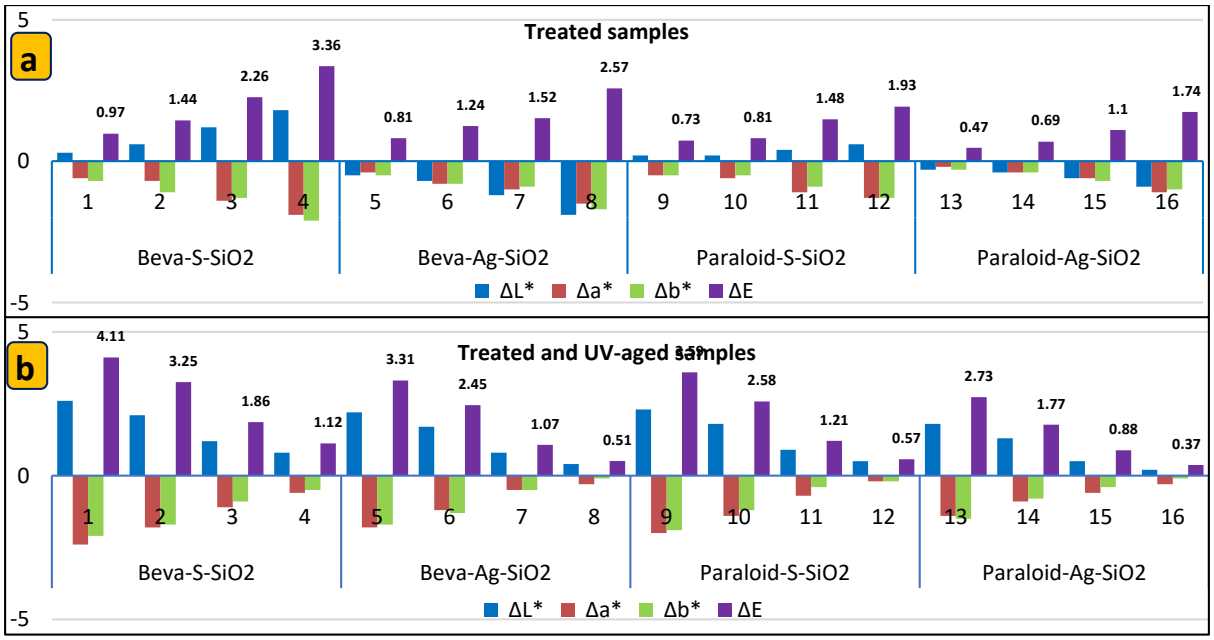

Fig. 4 Results of color difference of treated samples (a), and treated and UV-aged samples (b).

2.2.2.2. Air permeability and weight differences

The results of air permeability and weight differences between SFMs and SFMs-ABNCs before and after UV-aging revealed no remarkable difference in air permeability (Fig. 5a) or weight (Fig. 5b). They generally confirmed the suitability of proposed treatments due to less effect on fabric properties and keeping the physical properties of the silk fabric as normal ones (Al-Gaoudi et al., 2024; Ogulata, 2006). Ag-SiO_2 exhibited less air permeability after treatment with Paraloid and Beva. Due to the somewhat blocking of the micropores of the fabric by the acrylic-based nanocomposite, a decrease in the air permeability test of the silk fabric was observed (Gao et al., 2019). This finding generally matches the literature related to using any polymer-based nanomaterials (Ahmed et al., 2022; Al-Gaoudi et al., 2024; Mohammadipour-Nodoushan et al., 2023). Consequently, a relevant increase in the weight of fabric samples was observed.

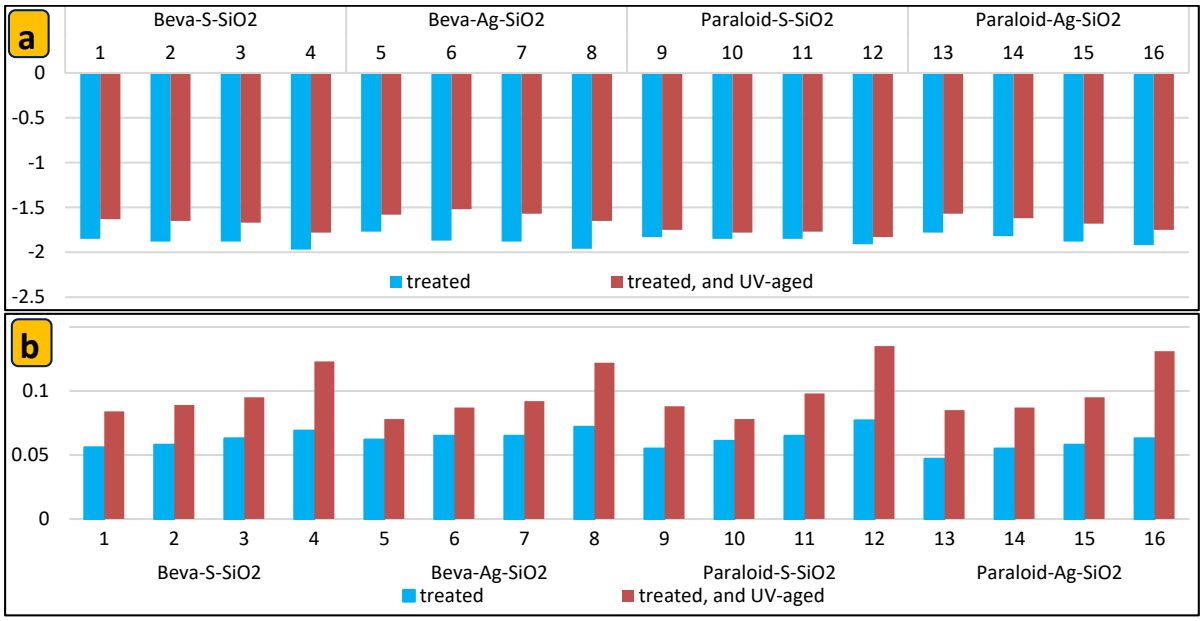

Fig. 5 results of air permeability difference (a), and weight difference (b) of treated samples, and treated and UV-aged samples

2.2.3. Antimicrobial activities

The results (Table 2 and Fig. 6) revealed that all treatments exhibited specific antimicrobial effects against all tested fungi and bacteria, particularly at the highest concentration (600 µg/mL), which had the most pronounced effect. The higher the concentration of nanomaterials, the larger the inhibition zone, which varied from 675 mm^2 (as the largest inhibition zone) in the case of Paraloid-Ag-SiO_2 against S. aureus, to 110 mm^2 (as the smallest inhibition zone) in the case of Beva-S-SiO_2 against P. fluorescens. Due to the Ag nanoparticles as an efficient antibacterial agent, the Ag-based nanocomposites exhibited more antimicrobial activities, especially in the case of *E. coli* and *S. aureus* (Tran et al., 2023; Ye et al., 2024). Moreover, the Ag-based nanocomposites exhibited an efficient antimicrobial activity against *Aspergillus* and *Penicillium* (El-Kadi et al., 2018b; Rehan et al., 2021). Sulfur-based nanocomposites exhibited good antimicrobial activities against gram-positive and gram-negative bacteria, especially *E. coli*, *S. aureus*, and *P. aeruginosa* (Dop et al., 2023; Kim et al., 2020), and fungi as well, especially *A. flavus* (Kim et al., 2020) in accordance with the literature. Sulfur-based nanocomposites exhibited higher antimicrobial activity against Gram-positive bacteria than against Gram-negative bacteria, which could be due to the method of preparation of sulfur nanoparticles, as suggested by the literature (Kim et al., 2020); consequently, it affected the sulfur-based nanocomposite.

 DOI: 10.21608/shedet.2025.386138.1302

Table 2. Antimicrobial activity by inhibition zone (mm^2) of different treatments.

Type	Name	Beva-S-SiO_2			Beva-Ag-SiO_2			Paraloid-S-SiO_2			Paraloid-Ag-SiO_2		
		200 µg/mL	400 µg/mL	600 µg/mL	200 µg/mL	400 µg/mL	600 µg/mL	200 µg/mL	400 µg/mL	600 µg/mL	200 µg/mL	400 µg/mL	600 µg/mL
Fungi	*A. niger*	165	302	465	395	476	576	174	226	288	410	568	650
	A. fumigatus	158	296	355	295	390	484	168	227	294	326	468	528
	C. halotolerans	126	170	215	176	195	225	165	208	246	155	208	256
	P. frequentans	153	194	255	185	275	325	155	192	245	181	290	366
	A. alternata	176	240	325	215	298	386	210	240	320	195	245	395
	R. oryzae	133	155	183	163	210	196	163	185	265	175	248	256
Gram (+) bacteria	*B. cereus*	147	180	225	345	472	552	179	238	317	390	575	625
	S. aureus	154	190	259	295	400	576	198	242	323	470	595	676
	S. albus	173	217	288	398	478	552	186	234	297	485	566	625
Gram (-) bacteria	*E. coli*	133	155	283	160	214	256	196	253	325	214	250	324
	P. aeruginosa	164	220	265	191	222	272	179	226	285	198	264	324
	P. fluorescens	110	174	230	190	293	400	126	196	242	323	400	484

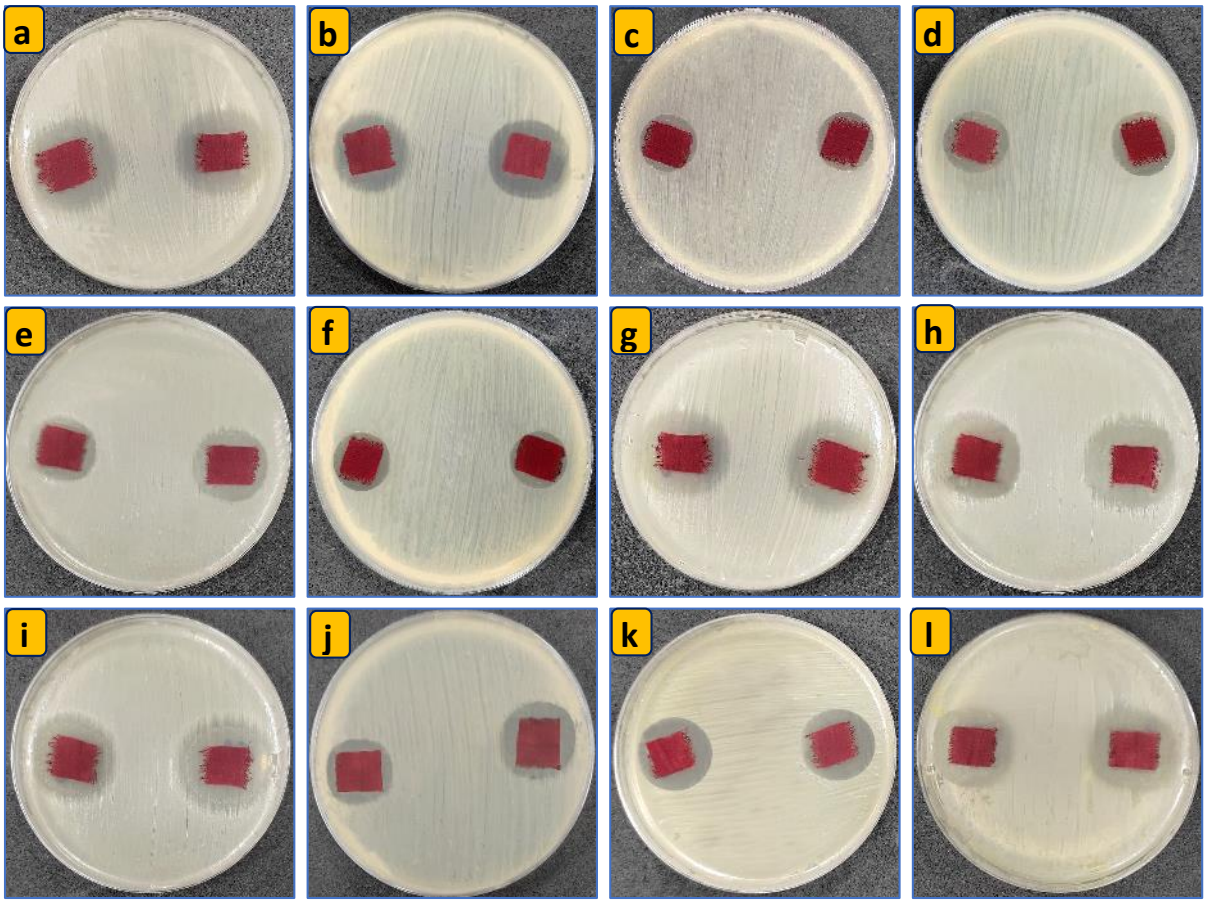

Fig. 6 Antimicrobial activity by inhibition zone (mm^2) of 600 µg/mL concentration of the top antimicrobial activities of both Beva-Ag-SiO_2 (left silk-fabric smple) and Paraloid-Ag-SiO_2 (right silk-fabric sample) *against A. niger* (a), *A. fumigatus* (b), *C. halotolerans* (c), *P. frequentans* (d), *A. alternata* (e), *R. oryzae* (f), *B. cereus* (g), *S. aureus* (h), *S. albus* (i), *E. coli* (j), *P. aeruginosa* (k), *P. fluorescens* (l).

3. CONCLUSIONS

Two nanocomposites (S-SiO_2 and Ag-SiO_2) were prepared, suspended, and sonicated in two acrylic co-polymers (Beva 371 and Paraloid B72) commonly used in the consolidation of

heritage materials, to assess the efficiency of these four acrylic-based nanocomposites in consolidation, UV-blocking, and antimicrobial activities against six fungi and six bacteria, applied on dyed silk-fabric samples. The obtained results confirmed the successful preparation of both nanocomposites, with a uniform size of ~50-80 nm. All treatments had varying effects, either positive or negative, on the different properties of silk-fabric samples. The more the concentration of nanomaterials, the more the effect on the properties of silk-fabric samples.

Paraloid-based treatments showed higher improvements in tensile strength, air permeability, weight, and color stability; on the contrary, Beva-based treatments exhibited better results with respect to the elongation% and flexibility of the samples. The Ag-based nanocomposites exhibited better results than S-based nanocomposites with respect to anti-UV and antimicrobial activities against different fungi and bacteria. Paraloid B72-Ag-SiO_2 acrylic-based nanocomposite (concentration of 600 µg/mL) is recommended as a multifunctional formula for consolidation, UV-blocking, and antimicrobial activity, to be applied to stiff or thick heritage textiles and carpets, due to its efficiency and minimal adverse effects on samples' properties, except stiffness. Beva 371-Ag-SiO_2 acrylic-based nanocomposite (concentration of 600 µg/mL) is recommended as a multifunctional formula for consolidation, UV-blocking, and antimicrobial activity to be applied to fine and delicate heritage textiles, due to its efficiency and less adverse effects on the stiffness of the silk-fabrics properties.

ACKNOWLEDGEMENT

The author would like to thank Prof. El-Hussien Moawad at the Faculty of Science, Dr. Khaled Syed-Ahmed, and Dr. Mohamed El-Rian at the Faculty of Agriculture, Damietta University, for their assistance with the preparation of nanomaterials and antimicrobial experiments for the study.

 DOI: 10.21608/shedet.2025.386138.1302

BIBLIOGRAPHY:

- Abdel-Kareem, O. (2010). Evaluating the combined efficacy of polymers with fungicides for protection of museum textiles against fungal deterioration in Egypt. *polish Journal of Microbiology*, *59*(4), 271-280.
- Abdel-Kareem, O. (2010). Monitoring, controlling and prevention of the fungal deterioration of textile artifacts in the museum of Jordanian heritage. *Mediterranean Archaeology and Archaeometry*, *10*(2), 85-96.
- Abdel-Kareem, O., Abdel-Rahim, H., Ezzat, I., & Essa, D. M. (2015). Evaluating the use of chitosan coated Ag nano-SeO2 composite in consolidation of Funeral Shroud from the Egyptian Museum of Cairo. *Journal of Cultural Heritage*, *16*(4), 486-495.
- Abdel-Kareem, O., & Nasr, H. (2010). Enhancing the long-term durability of historical wool textiles using water dispersed nano polymers. *Journal of American Science*, *6*(10), 1186-1194.
- Abou Abou Rida, M., & Harb, F. (2014). Synthesis and characterization of amorphous silica nanoparitcles from aqueous silicates uisng cationic surfactants. *Journal of Metals, Materials and Minerals*, *24*(1).
- Ahmed, H. E., Marouf, S., & Mohamed, W. S. (2022). Antifungal activity assessment of nanocomposites of natural chitosan and gelatin with a mahogany plant extract for conservation of historical textiles. *Heritage Science*, *10*(1), 198.
- Al-Gaoudi, H. A., Marouf, M. A., Badry, N., & Rehan, M. (2024). A facile approach to developing multifunctional archaeological wool fabric surface with self-cleaning, and UV protection properties using nano-coating. *Inorganic Chemistry Communications*, *167*, 112716.
- Aldoasri, M. A., Darwish, S., Mahmoud, A., Elmarzugi, N., & Sayed, A. (2018). Performance of Clay, SiO2, Ca (OH) 2 and CaCO3-polymeric nanocomposites for conservation and preservation of limestone artworks. *Preprints*.
- Alrefaee, S. H., Sefrji, F. O., Obaid, R., Alsharari, A. M., Mojally, M., Alisaac, A.,…El-Metwaly, N. M. (2024). Rosmarinus officinalis-based Ag/SiO2 and CeO2-Ag/SiO2 core-shell nanocomposites: A green approach to phytochemical analyses, molecular docking, antioxidant and antimicrobial applications with enhanced biocompatibility. *Results in Engineering*, *24*, 103478.
- Anna, W., Dorota, R., Mansur, R., & Sławomir, W. (2020). Microorganisms colonising historical cardboard objects from the Auschwitz-Birkenau State Museum in Oświęcim, Poland and their disinfection with vaporised hydrogen peroxide (VHP). *International Biodeterioration & Biodegradation*, *152*, 104997.
- Bechtold, T., Turcanu, A., Ganglberger, E., & Geissler, S. (2003). Natural dyes in modern textile dyehouses—how to combine experiences of two centuries to meet the demands of the future? *Journal of Cleaner Production*, *11*(5), 499-509.
- Bratasz, Ł., Łukomski, M., Klisińska-Kopacz, A., Zawadzki, W., Dzierżęga, K., Bartosik, M.,…Kozłowski, R. (2015). Risk of Climate-Induced Damage in Historic Textiles. *Strain*, *51*(1), 78-88.
- Brimblecombe, P., & Lankester, P. (2013). Long-term changes in climate and insect damage in historic houses. *Studies in Conservation*, *58*(1), 13-22.
- Brzozowska, I., Bogdanowicz, A., Szczęsny, P., Zielenkiewicz, U., & Laudy, A. (2018). Evaluation of bacterial diversity on historical silk velvet textiles from the Museum of King John III's Palace at Wilanów, Poland. *International Biodeterioration & Biodegradation*, *131*, 78-87.
- Błyskal, B. (2015). Fungal deterioration of a woollen textile dyed with cochineal. *Journal of Cultural Heritage*, *16*(1), 32-39.
- Cai, T., Ge-Zhang, S., Zhang, C., Mu, P., & Cui, J. (2024). Excellent Antibacterial Properties of Silver/Silica–Chitosan/Polyvinyl Alcohol Transparent Film. *International Journal of Molecular Sciences*, *25*(15), 8125.

- Ching, Y. C., Rahman, A., Ching, K. Y., Sukiman, N. L., & Cheng, H. C. (2015). Preparation and characterization of polyvinyl alcohol-based composite reinforced with nanocellulose and nanosilica. *BioResources*, *10*(2), 3364-3377.
- De Leo, F., & Isola, D. (2023). *The Role of Fungi in Biodeterioration of Cultural Heritage: New Insights for Their Control*. MDPI-Multidisciplinary Digital Publishing Institute.
- De Witte, E. (1982, 21st-22nd May 1982). Resins in conservation-introduction to their properties and applications.*The proceedings of the symposium resins in conservation* In *The proceedings of the symposium resins in conservation*, Edinburgh.
- Degani, L., Gulmini, M., Piccablotto, G., Iacomussi, P., Gastaldi, D., Dal Bello, F., & Chiantore, O. (2017). Stability of natural dyes under light emitting diode lamps. *Journal of Cultural Heritage*, *26*, 12-21.
- del Carmen Calvo, A. M., Docters, A., Miranda, M. V., & Saparrat, M. C. N. (2017). The use of gamma radiation for the treatment of cultural heritage in the Argentine National Atomic Energy Commission: past, present, and future. *Applications of Radiation Chemistry in the Fields of Industry, Biotechnology and Environment*, 227-247.
- Dhanalekshmi, K. I., Magesan, P., Sangeetha, K., Zhang, X., Jayamoorthy, K., & Srinivasan, N. (2019). Preparation and characterization of core-shell type Ag@ SiO2 nanoparticles for photodynamic cancer therapy. *Photodiagnosis and photodynamic therapy*, *28*, 324-329.
- Dop, R. A., Neill, D. R., & Hasell, T. (2023). Sulfur-polymer nanoparticles: preparation and antibacterial activity. *ACS Applied Materials & Interfaces*, *15*(17), 20822-20832.
- El-Kadi, S. M., Mahmoud, M. K., Sayed-Ahmed, K., & El-Hendawy, M. A. (2018a). Comparison between silver nanoparticles and silver nitrate as antifungal agent. *International Journal of Nanoscience and Nanoengineering*, *4*(1), 5-11.
- El-Kadi, S. M., Mahmoud, M. K., Sayed-Ahmed, K. A., & El-Hendawy, M. A. (2018b). Comparison between silver nanoparticles and silver nitrate as antifungal agent. *International Journal of Nanoscience and Nanoengineering*, *4*(1), 5-1.
- Elkadi, H., Al-Maiyah, S., Fielder, K., Kenawy, I., & Martinson, D. B. (2021). The regulations and reality of indoor environmental standards for objects and visitors in museums. *Renewable and Sustainable Energy Reviews*, *152*, 111653.
- Elsayed, Y. (2025). Application of a Multi-Functional Acrylic Based Varnish Reinforced with Nanoparticles in the Preservation of Oil Paintings. مجلة كلية الآثار. جامعة القاهرة، ١٨(٢٨)، ٣٧٥-٣٩٥.
- Elsayed, Y., El-Kadi, S., El-Rian, M., & Mabrouk, N. (2023). The efficiency of microbial culture extracts as green antimicrobial products against some microorganisms colonizing the historic oil paintings. *Scientific Culture*, *9*(2), 127-143.
- Elsayed, Y., & Sayed-Ahmed, K. (2024). A Novel Approach of Using Green Synthesized Tellurium Nanoparticles to Protect Historical Oil Paintings from Bacterial Degradation. *Shedet*, *13*(13).
- Emamhadi, M. A., Sarafraz, M., Akbari, M., Thai, V. N., Fakhri, Y., Linh, N. T. T., & Khaneghah, A. M. (2020). Nanomaterials for food packaging applications: A systematic review. *Food and Chemical Toxicology*, *146*, 111825.
- Ezz Eldeen, H., Mohamed, W. S., Saad, H., Mahmoud, N., & Radi, R. (2020). A Comparative Study of the Impact of Beva 371 and Nano Vinyl Acetate Derivatives on Textiles Properties for Historical Textiles Conservation, Practical Application. *Egyptian Journal of Chemistry*, *63*(4), 1383-1396.
- Forlani, G., Seves, A. M., & Ciferri, O. (2000). A bacterial extracellular proteinase degrading silk fibroin. *International biodeterioration & biodegradation*, *46*(4), 271-275.
- Gao, D., Li, Y., Lyu, B., Lyu, L., Chen, S., & Ma, J. (2019). Construction of durable antibacterial and anti-mildew cotton fabric based on P (DMDAAC-AGE)/Ag/ZnO composites. *Carbohydrate polymers*, *204*, 161-169.

 DOI: 10.21608/shedet.2025.386138.1302

- Goodarzian, H., & Ekrami, E. (2010). Extraction of dye from madder plant (Rubia tictorium L.) and dyeing of wool.
- Grifoni, D., Bacci, L., Zipoli, G., Albanese, L., & Sabatini, F. (2011). The role of natural dyes in the UV protection of fabrics made of vegetable fibres. *Dyes and Pigments*, *91*(3), 279-285.
- Guo, C., Lan, L., Liu, Y., Meng, N., & Li, C. (2023). Comparison of environmental criteria for conservation and storage of collections: A comprehensive literature review. *Building and Environment*, *243*, 110665.
- Gutarowska, B., Pietrzak, K., Machnowski, W., & Milczarek, J. M. (2017). Historical textiles–a review of microbial deterioration analysis and disinfection methods. *Textile Research Journal*, *87*(19), 2388-2406.
- International, A. (2004). *Annual book of ASTM standards*. ASTM international.
- Ion, R.-M., & Grigorescu, R.-M. (2018). Polymeric Micro-and Nanosystems for Wood Artifacts. *New Uses of Micro and Nanomaterials*, 73.
- Jia, M., Zhang, X., Weng, J., Zhang, J., & Zhang, M. (2019). Protective coating of paper works: ZnO/cellulose nanocrystal composites and analytical characterization. *Journal of cultural heritage*, *38*, 64-74.
- Johansson, S., Wadsö, L., & Sandin, K. (2010). Estimation of mould growth levels on rendered façades based on surface relative humidity and surface temperature measurements. *Building and Environment*, *45*(5), 1153-1160.
- Kakakhel, M. A., Wu, F., Gu, J.-D., Feng, H., Shah, K., & Wang, W. (2019). Controlling biodeterioration of cultural heritage objects with biocides: A review. *International Biodeterioration & Biodegradation*, *143*, 104721.
- Kavkler, K., Cimerman, N. G., Zalar, P., & Demšar, A. (2015). Deterioration of contemporary and artificially aged cotton by selected fungal species. *Polymer Degradation and Stability*, *113*, 1-9.
- Kavkler, K., Gunde-Cimerman, N., Zalar, P., & Demšar, A. (2014). Fungal deterioration of aged textiles. *Nova Science Publishers: New York, NY, USA*, 315-342.
- Kim, Y. H., Kim, G. H., Yoon, K. S., Shankar, S., & Rhim, J.-W. (2020). Comparative antibacterial and antifungal activities of sulfur nanoparticles capped with chitosan. *Microbial Pathogenesis*, *144*, 104178.
- Krejčí, J., Drábková, K., Bureš Víchová, J., & Škrdlantová, M. (2021). Reversibility of adhesive techniques applied on historical textiles. *The European Physical Journal Plus*, *136*(6), 642.
- Liu, T., Zhang, Y., Li, C.-H., Marquez, M. D., Tran, H.-V., Robles Hernández, F. C.,…Lee, T. R. (2020). Semihollow Core–Shell Nanoparticles with Porous SiO2 Shells Encapsulating Elemental Sulfur for Lithium–Sulfur Batteries. *ACS Applied Materials & Interfaces*, *12* (42), 47368-47376.
- Lucchi, E. (2018). Review of preventive conservation in museum buildings. *Journal of Cultural Heritage*, *29*, 180-193.
- Maekawa, S., Beltran, V. L., & Henry, M. C. (2015). *Environmental Management for Collections: Alternative Conservation Strategies for Hot and Humid Climates*, Getty Publications.
- Mahović Poljaček, S., Tomašegović, T., Leskovšek, M., & Stanković Elesini, U. (2021). Effect of SiO2 and TiO2 nanoparticles on the performance of UV visible fluorescent coatings. *Coatings*, *11*(8), 928.
- Mandal, S., Kumar, P., Satpathy, B., Das, K., & Das, S. (2024). Nanostructured metal oxide based coating for the protection and conservation of cultural heritage: A comprehensive review. *Journal of Cultural Heritage*, *69*, 94-112.

_ Marchiafava, V., Bartolozzi, G., Cucci, C., De Vita, M., & Picollo, M. (2014). Colour measurements for monitoring the conservation of contemporary artworks. *JAIC-Journal of the International Colour Association*, *13*, 36-42.

_ Michalski, S. (2018). Agent of deterioration: light, ultraviolet and infrared. *Canadian Conservation Institute*, *17*.

_ Mitani, A., Kamperidou, V., & Terzopoulou, P. (2024). Surface Treatment of Oak Wood with Silica Dioxide Nanoparticles and Paraloid B72. *Forests*, *15*(11), 1842.

_ Mohammadipour-Nodoushan, R., Shekarriz, S., Shariatinia, Z., Heydari, A., & Montazer, M. (2023). Improved cotton fabrics properties using zinc oxide-based nanomaterials: a review. *International Journal of Biological Macromolecules*, *242*, 124916.

_ Montegut, D., Indictor, N., & Koestler, R. J. (1991). Fungal deterioration of cellulosic textiles: a review. *International biodeterioration*, *28*(1-4), 209-226.

_ Morones, J. R., Elechiguerra, J. L., Camacho, A., Holt, K., Kouri, J. B., Ramírez, J. T., & Yacaman, M. J. (2005). The bactericidal effect of silver nanoparticles. *Nanotechnology*, *16*(10), 2346.

_ Municchia, A. C., Bartoli, F., Taniguchi, Y., Giordani, P., & Caneva, G. (2018). Evaluation of the biodeterioration activity of lichens in the Cave Church of Üzümlü (Cappadocia, Turkey). *International Biodeterioration & Biodegradation*, *127*, 160-169.

_ Nugari, M. P., & Salvadori, O. (2017). Biodeterioration control of cultural heritage: Methods and products. In *Molecular biology and cultural heritage* (pp. 233-242). Routledge.

_ Ogulata, R. T. (2006). Air permeability of woven fabrics. *Journal of Textile and Apparel, Technology and management*, *5*(2), 1-10.

_ Oriola-Folch, M., Campo-Francés, G., Nualart-Torroja, A., Ruiz-Recasens, C., & Bautista-Morenilla, I. (2020). Novel nanomaterials to stabilise the canvas support of paintings assessed from a conservator's point of view. *Heritage Science*, *8*(1), 23.

_ Palladino, N., Hacke, M., Poggi, G., Nechyporchuk, O., Kolman, K., Xu, Q.,…Baglioni, P. (2020). Nanomaterials for combined stabilisation and deacidification of cellulosic materials—the case of iron-tannate dyed cotton. *Nanomaterials*, *10*(5), 900.

_ Perkas, N., Amirian, G., Dubinsky, S., Gazit, S., & Gedanken, A. (2007). Ultrasound-assisted coating of nylon 6, 6 with silver nanoparticles and its antibacterial activity. *Journal of applied polymer science*, *104*(3), 1423-1430.

_ Princi, E., Vicini, S., Pedemonte, E., Arrighi, V., & McEwen, I. (2005). New polymeric materials for paper and textile conservation. I. Synthesis and characterization of acrylic copolymers. *Journal of applied polymer science*, *98*(3), 1157-1164.

_ Rai, M., Ingle, A. P., & Paralikar, P. (2016). Sulfur and sulfur nanoparticles as potential antimicrobials: from traditional medicine to nanomedicine. *Expert review of anti-infective therapy*, *14*(10), 969-978.

_ Ramasamy, F. (2019). A review on the investigation of biologically active natural compounds on cotton fabrics as an antibacterial textile finishing. *International Research Journal of Science and Technology*, *1*(1), 49-55.

_ Ranakoti, L., Gangil, B., Rajesh, P. K., Singh, T., Sharma, S., Li, C.,…Mahmoud, O. (2022). Effect of surface treatment and fiber loading on the physical, mechanical, sliding wear, and morphological characteristics of tasar silk fiber waste-epoxy composites for multifaceted biomedical and engineering applications: fabrication and characterizations. *journal of materials research and technology*, *19*, 2863-2876.

_ Rehan, M., El-Naggar, M. E., Al-Enizi, A. M., Alothman, A. A., Nafady, A., & Abdelhameed, R. M. (2021). Development of silk fibers decorated with the in situ synthesized silver and gold nanoparticles: antimicrobial activity and creatinine adsorption capacity. *Journal of Industrial and Engineering Chemistry*, *97*, 584-596.

 DOI: 10.21608/shedet.2025.386138.1302

- Ruparelia, J. P., Chatterjee, A. K., Duttagupta, S. P., & Mukherji, S. (2008). Strain specificity in antimicrobial activity of silver and copper nanoparticles. *Acta biomaterialia*, *4*(3), 707-716.
- Sadek, M. E., Shabana, Y. M., Sayed-Ahmed, K., & Abou Tabl, A. H. (2022). Antifungal activities of sulfur and copper nanoparticles against cucumber postharvest diseases caused by Botrytis cinerea and Sclerotinia sclerotiorum. *Journal of Fungi*, *8*(4), 412.
- Samadelli, M., Zink, A. R., Roselli, G., Gabrielli, S., Tabandeh, S., & Fernicola, V. C. (2019). Development of passive controlled atmosphere display cases for the conservation of cultural assets. *Journal of Cultural Heritage*, *35*, 145-153.
- Schanda, J. (2007). *Colorimetry: understanding the CIE system*. John Wiley & Sons.
- Scheerer, S., Ortega-Morales, O., & Gaylarde, C. (2009). Microbial deterioration of stone monuments—an updated overview. *Advances in applied microbiology*, *66*, 97-139.
- Schweppe, H. (1988). Practical information for the identification of dyes on historic textile materials.
- Sengupta, S., Debnath, S., & Sengupta, A. (2016). Fabric bending behaviour testing instrument for technical textiles. *Measurement*, *87*, 205-215.
- Seves, A., Romanò, M., Maifreni, T., Sora, S., & Ciferri, O. (1998). The microbial degradation of silk: a laboratory investigation. *International biodeterioration & biodegradation*, *42*(4), 203-211.
- Singer, H., Jaus, S., Hanke, I., Lück, A., Hollender, J., & Alder, A. C. (2010). Determination of biocides and pesticides by on-line solid phase extraction coupled with mass spectrometry and their behaviour in wastewater and surface water. *Environmental pollution*, *158*(10), 3054-3064.
- Szostak-Kotowa, J. (2004). Biodeterioration of textiles. *International Biodeterioration & Biodegradation*, *53*(3), 165-170.
- Sülar, V., & Devrim, G. (2019). Biodegradation behaviour of different textile fibres: visual, morphological, structural properties and soil analyses. *Fibres & Textiles in Eastern Europe*, *27*(1 (133)).
- Tran, N. T., Ha, D., Pham, L. H., Vo, T. V., Nguyen, N. N., Tran, C. K.,…Nguyen, P. L. M. (2023). Ag/SiO2 nanoparticles stabilization with lignin derived from rice husk for antifungal and antibacterial activities. *International Journal of Biological Macromolecules*, *230*, 123124.
- Tétreault, J. (2003). Airborne pollutants in museums, galleries and archives: risk assessment, control strategies and preservation management.
- Vasileiadou, A., Karapanagiotis, I., & Zotou, A. (2022). A chromatographic investigation on ageing of natural dyes in silk under UV light. *Archaeological and Anthropological Sciences*, *14*(1), 21.
- Vilaplana, F., Nilsson, J., Sommer, D. V. P., & Karlsson, S. (2015). Analytical markers for silk degradation: comparing historic silk and silk artificially aged in different environments. *Analytical and bioanalytical chemistry*, *407*(5), 1433-1449.
- Yasuda, K., Okazaki, Y., Abe, Y., & Tsuga, K. (2017). Effective UV/Ozone irradiation method for decontamination of hydroxyapatite surfaces. *Heliyon*, *3*(8).
- Ye, L., Li, H., Xiang, J., Chen, J., Zhang, X., Zheng, S., & Liao, W. (2024). Synthesis of Ag@ SiO2 core-shell nanoparticles for antibacterial application in water-based acrylic polymer coatings. *Surfaces and Interfaces*, *51*, 104490.
- Yong-hua, R., Bian-xia, L., & Xiao-ning, S. (2012). Research on the Aging of Natural Fiber Textiles. *Advances in Biomedical Engineering*, *9*, 1.

استخدام مركبات نانوية متعددة الوظائف قائمة على الأكريليك لحماية المنسوجات التراثية

نبيل مبروك

كلية الآثار جامعة دمياط

nsh00@du.edu.eg

بيانات المقال

تاريخ المقال

تم الاستلام في ١٠ ديسمبر ٢٠٢٤

تم استلام النسخة المنقحة في ٧ فبراير ٢٠٢٥

تم قبول البحث في ٢٨ فبراير ٢٠٢٥

متاح على الإنترنت في ١٨ يونيه ٢٠٢٥

الكلمات الدالة

Ag-SiO2

S-SiO2

متعدد الوظائف؛

مركب نانوي؛

منسوجات تراثية؛

الملخص

تهدف الدراسة إلى تقييم كفاءة مركبين نانويين (S-SiO2 و-Ag SiO2)معلقين في كوبوليمرين (بيفا٣٧١ و بارالويد ب٧٢) في تقوية، وحجب أشعة UV ومقاومة الميكروبات ضد ستة من الفطريات وستة من البكتيريا، مطبقة على عينات قماش حرير مصبوغ. للدراسة استخدمت تقنيات TEM و SEM-EDX و XRD و UTM ومقياس اللون وجهاز اختبار الصلابة ونفاذية الهواء ووزن العينات ومساحة تثبيط الميكروبات. أكدت النتائج التحضير الناجح لكلا المركبين النانويين. تسببت جميع المعالجات في تأثيرات متباينة، إيجابية أو سلبية، على خصائص عينات القماش. فكلما زاد تركيز المواد النانوية زاد التأثير على خصائص العينات. أظهرت المعالجات القائمة على البارالويد ب٧٢ تحسنًا أكبر في جميع خصائص العينات، ولكنها زادت الصلابة. على العكس من ذلك، أظهرت المعالجات القائمة على بيفا٣٧١ نتائج أفضل في نسبة الاستطالة والمرونة. أظهرت المعالجات القائمة على الفضة نتائج أفضل من المعالجات القائمة على الكبريت في نشاطها ضد أشعة UV والفطريات والبكتيريا محل الدراسة. توصي الدراسة باستخدام تركيز ٦٠٠ µg/mL من مركب Ag-SiO2 النانوي المعلق في ٢% بارالويد ب٧٢ في التولوين كتركيبة متعددة الوظائف للتقوية وحجب أشعة UV ومقاومة الميكروبات في المنسوجات والسجاجيد التراثية الصلبة و/أو السميكة. بينما يُنصح باستخدام تركيز ٦٠٠ µg/mL من مركب Ag-SiO2 النانوي المعلق في ٢% من بيفا٣٧١ في التولوين كتركيبة متعددة الوظائف للمنسوجات التراثية الرقيقة.

 DOI: 10.21608/shedet.2025.386138.1302